Thermal Expansion Coefficient Measurement of Solid Materials by Displacement Sensor System Based on Virtual Instrument Technology

Zakaryae Ezzouine[1], Abdelrhani Nakheli[2]

[1]Department of physics, LASMAR, Faculty of Sciences, Moulay Ismail University, Meknes, Morocco
[2]Department of Electrical Engineering, ESTM, Faculty of Science, Moulay Ismail University, Meknes, Morocco

Abstract— *The coefficient of linear thermal expansion is a physical property of the material that is indicative of the extent to which a material expands when it is heated. This article describes a fast technique uses a new tool based on an inductive displacement sensor (IDS) connected to a sample material for test (rod or test tube) for measurement of the linear thermal expansion of metals. By this technique the sample is normally inserted in a special liquid bath (thermostat) to obtain the temperatures required. The rod is attached to the bath by a mounting bracket, and then we heat it by a heating resistor. Under the temperature effect, the rod expands to its free extremity and causes a displacement detected by the IDS which allows converting this displacement into a voltage by the intermediate of an electronic card. We have also developed a graphical user interface (GUI) by utilizing LabVIEW software for acquire and display the information obtained by the experimental set-up. The GUI controlling program can be used to determine the Coefficient of Linear Thermal Expansion of metals with acceptable accuracy.*

Keywords— Inductive displacement sensor, linear thermal expansion, LabVIEW, Data acquisition, Graphical user interface (GUI).

I. INTRODUCTION

The material contains atoms or molecules which are agitated under the temperature’s effect. When the temperature is increased, most materials undergo an augmentation of their volume. This expansion appears microscopically. So, that’s what we call dilatation. By contrast, when the temperature is decreased, they are contracted. This property is observed in all material’s status, but it is not always visible [1-3]. Historically, the conventional means for measuring expansion coefficients are the "dilatometer", “high magnification optical imaging”, "thermo-mechanical analysis», Strain gauge ,"Laser Interferometer”[4-14]. The dilatation is expressed by the thermal expansion coefficient related to the nature of the studied material. For an isotropic material, that is to say, possesses an identical behavior towards all the space directions we can express this coefficient by formula in the following figure [15-18]:

The purpose of this paper is to present an experimental set-up for performing expansion and deformation tests on test tube. Its basic principle can be described as follows: a metallic rod is fixed to its end lower, whereas its free extremity is connected to the IDS in a thermostat. While the temperature is changed, the length of the rod section is varying by micrometer.

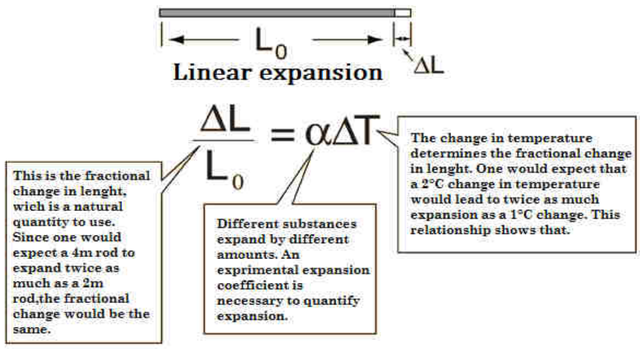

Fig. 1: General definition of thermal expansion coefficient

This variation is precisely measured by our system. The aims of this works is to demonstrate a fast technique with an IDS for thermal expansion coefficient measurement with a graphical user interface for visualization and aqcuisition data in real-time using DAQ (NI USB-6281) board and LabVIEW program software.

II. DESCRIPTION OF THE INDUCTIVE SENSOR ELEMENTS

2.1 Principle of operation

The proposed sensor is a displacement inductive sensor (IDS), as shown in Fig.2. Its operating principle is based on the phenomenon of influence with magnetic induction between two flat coils of the same diameter and having the same number of turns, located at a distance, x, from one another, on the same axis passing through their centers. One of the coils is attached to a horizontal support and powered with a low frequency generator, with specific phase conditions and amplification, this coil generates a sinusoidal voltage of 16 kHz and amplitude of 2V. The second flat coil is wound on a cylinder isolate, connected to the extremity of a spring. The other extremity of the same spring is hooked to a fixed support [19-16].

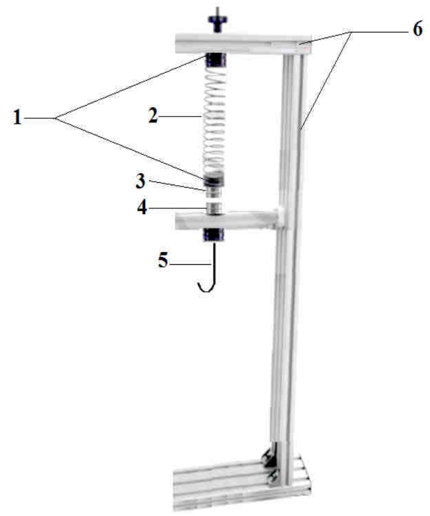

Fig. 2: Displacement inductive sensor: 1, Guide cylinder; 2, calibrated spring; 3, Receiver coil (Moving coil); 4, Transmitter coil; 5, Hook

The second coil is secured to the cylinder suspended vertically in spring. The two coils, the spring and the cylinder are aligned on the same vertical axis. The cylinder acts as a guide, since it can move vertically and passes through an opening on the outline surrounding the fixed coil up or down, virtually without friction when exerts a force at its lower end; This has the effect of lengthening or compressing the spring.

The winding of the stationary coil is driven with a sinusoidal signal, it is passed through by a variable current (a variation of the velocity of the electrons), and thus an electric field must exist in the direction of the coil wire creating a magnetic induction variable along its axis (Fig.3).

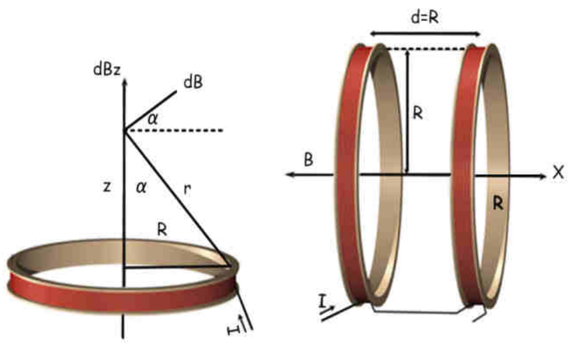

Fig. 3: Illustration of coil conductivity principle

This induction produces a variable flux Φ and a variable induced electromotive force on the electrons of the other coil (moving coil) equal to [19-23]:

$$e = -\frac{d\Phi}{dt} \tag{1}$$

The maximum value of the induced electromotive force depends on the distance z between the two coils, and the flow Φ is proportional to the magnetic induction B, variations, depending on z, is given by:

$$dB = \frac{\mu_0 \times N \times I}{4\Pi \times (r^3 \times dl^{\wedge r})} \tag{2}$$

$$dB = \frac{\mu_0 \times N \times I}{4\Pi \times (r^2 \times dl)} \tag{3}$$

$$dB(z) = dBSin\ \alpha = dB\ {}^{R}\!/_{r} \tag{4}$$

$$dB(z) = \frac{\mu_0 \times N \times I \times R}{4\Pi \times (r^3 \times dl)} \tag{5}$$

By symmetry, it is clear that B is parallel to z so B is the integral of

$$dB(z) = \frac{\mu_0 \times N \times I \times R}{4\Pi \times (r^3 \times dl)} \tag{6}$$

Is constant in the integral dB (z) reduces to the integral of dl on the circle which is so obviously 2πR:

$$B(z) = \frac{\mu_0 \times N \times I \times R^2}{2\Pi \times (r^3)} \tag{7}$$

with $r = (R^2 + z^2)^{½}$

This gives:

$$B(Z) = \frac{\mu_0 \times N \times I \times R^2}{2 \times (R^2 + Z^2)^{3/2}} \tag{8}$$

I with the current flowing through the coils, their radius R, the number of turns N, and z is the distance between the two coils. For z = 0, the above formula is simple:

$$B(0) = \frac{\mu_0 \times N \times I}{2R} \tag{9}$$

When coupling a mass to the hook, the spring is extended, the cylinder moves downwards, and thus, the distance z between the two coils decreases; which results in an increase in the maximum induced voltage across the moving coil. The use of the spring, which acts as a force-displacement converter, allows using the sensor as a force sensor.

2.2 Performance and characteristics of the sensor

Sensor Drift: When we turn the sensor on, the output voltage decreases exponentially and after 15 minutes of operation, this voltage stabilizes at a characteristic constant of the experimental device.

Sensitivity: The sensitivity of the sensor depends on the spring constant of the spring used and conditioning circuit (particularly the gain of the amplifier stages), we achieved a sensitivity of 4mg/mV at the beginning (before suspending masses). However, the electromagnetic unit consisting of transmitter and receiver coil may be modified to increase the sensor sensitivity. In general, inductive sensors were first used for historical reasons, but are still interesting because of their accuracy and robustness. In addition, the coils are cheap and easy to produce industrially, at least within reasonable dimensions. The induction of a coil is directly related to its number of turns, its diameter and thus its size; the small coils generally have a lower sensitivity. However, advanced techniques now allow the production of coils of small size with high sensitivity, with complex shapes or a larger number of turns. The frequency domain for an inductive sensor depends strongly of its impedance.

Measuring Range: From 0g to 3 g, it's related to the mechanical properties of the spring. The sensor is designed to work in a range of 0 to 3g.

Accuracy: The accuracy of the sensor depends, obviously, on its own elements (coils, friction, inter coil distance, number of turns, spring, and the signal conditioning circuit), and the quality of the measuring apparatus used. The voltmeter used gives tension to an accuracy of 0.1mV. The reading error is estimated at 0.05 mV, and the result is an error Δm = 0.4 mg to 0g under the best conditions, and can reach 0.25 mg to 3g.

Hysteresis: We have made measurement on the sensor by hooking increasingly masses of 0g to 3 g per 1g in steps of 1g, and then we note the output voltage values by removing masses in steps of 1g. The results are perfectly reversible and there was no hysteresis cycle due to the mechanical properties of the spring which acts as a force-displacement converter. We were limited to a maximum weight of 3g, and beyond, there is a small deformation appearing. The choice of a good spring (perfectly elastic) is important. The spring constant of the spring used is k=1g/mm.

2.3 The Conditioning Circuit

The out voltage of sensor has very low amplitude, it was necessary to bring a conditioning circuit containing amplification stages, recovery and filtering, to make this voltage workable.

As shown in Figure 4, 5and 6 the conditioning circuit of liquid-level monitoring signal path has three stages. For that reason, stabilizing and increasing the out sensor voltage requires several processes.

The first step is finding the gain of the amplifier and multiplying this gain with the sensor voltage, finding the gain of an amplifier stage can be cumbersome.

Figure 4 shows a non-Inverting gain amplifier using an op amp. It presents high impedance to the sensor (at V_{SENSOR}) and produces a positive gain from V_{SENSOR} to V1. (Fig. 4) used in the application can be seen in equations 10 and 11.

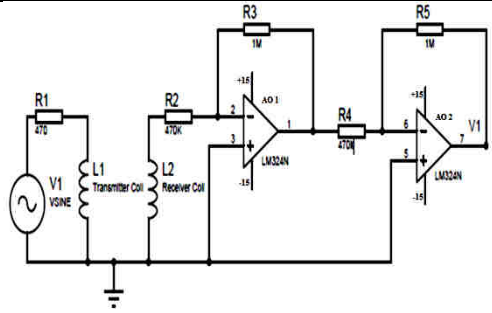

Fig. 4: Non-inverting Gain Amplifier for High-Impedance Sensors with Voltage Output.

$$V_{opAmp\,1} = \frac{R_2}{R_1} V_{SENSOR} \qquad (10)$$

$$V_{opAmp\,2} = V_1 = \frac{R_4}{R_3} \times \frac{R_2}{R_1} V_{sensor} \qquad (11)$$

The circuit shown in Figure 5 is composed of a full-wave rectifier circuit, a low-pass RC filter followed by an operational amplifier, the closed loop gain is:

$$ACL = \frac{R8}{R9} + 1 \qquad (12)$$

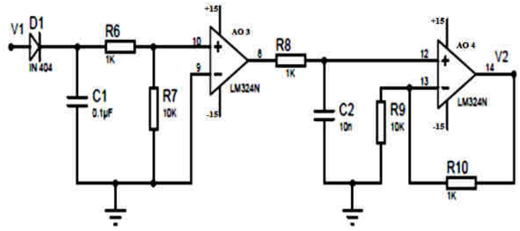

Fig. 5: Full-wave rectifier circuit and Low Pass Butterworth Filter

The function of the IDS as described in the preceding paragraph, when the inter coil distance decreases the output voltage becomes maximum, so for detecting the ascent and descent of liquid, a differentiator is added to reverse the sensor behavior.

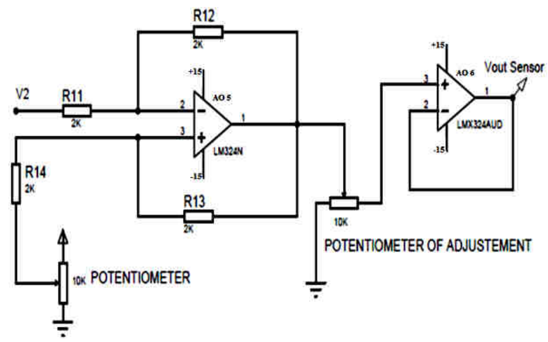

Fig. 6: Differentiator circuit and potentiometer for adjustment

The resistor values of differentiator circuit are equal; this amplifier will have a differential voltage gain of 1. The analysis of this circuit is essentially the same as that of an inverting amplifier ‹Therefore:

$$V_{OUTdifferentiator} = V_{potentiometer} - V_2 \qquad (13)$$

The conditioning circuit also includes an adjustable control potentiometer resistor used to adjust the sensitivity of sensor.

III. EXPERIMENTAL SETUP

The experimental setup design for thermal expansion measurement based on the IDS is shown in Fig. 8.

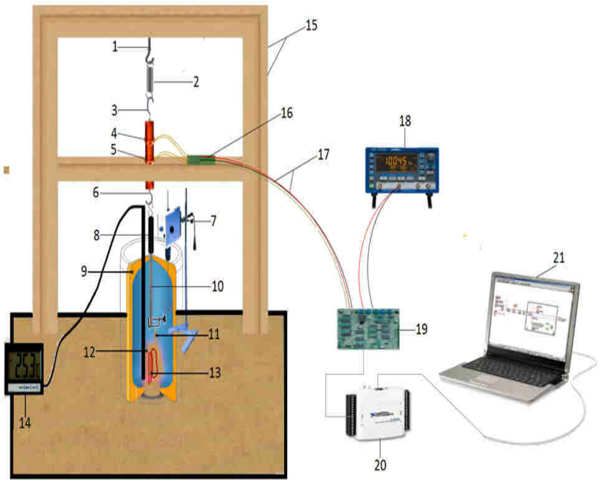

*Fig. 8: Exprimental setup for measuring of the thermal expansion coefficient: **1**, Hook; **2**, spring; **3**, Hook; **4**, Moving coil; **5**, Fixed coil; **6**, Hook; **7**,Agitator;**8**,Fixation cylinder;**9**,Insulating foam;**10**,Test Tube fixed by a Mounting bracket in lower extremity; **11**,Magnesium anode; **12**,Thermostat; **13**,Heating resistor; **14**,Thermometer;**15**, Fixed support ; **16**,Printed circuit board ;**17**,wire connections ;**18**,Low frequency generator ;**19**,conditing circuit ;**20**, Acquisition card ;**21**, computer [29].*

The technique of obtaining thermal expansion coefficient marked by the device is a thermal analysis technique that measures the expansion or contraction of a solid material; the two essential parameters are temperature and time. To measure the linear thermal expansion is used the device above. The device is technologically close of the first measuring instruments used in this field.

The operation of the instrument is simple to understand. The sample is placed in the center, built at one end, at the other. The rod is then heated with the heating resistor placed immediately below, and then expands. The sensor located at the free end is initially in contact with the rod before the linear expansion starts. The expansion is then read as variations in the voltage of the sensor out, tensions must be processed on the go with the calibration curve, this instrument can detect changes in length with all types of solid metals.

IV. RESULTS AND DISCUSSION

3.1 Sensor Calibration

The characteristic curve of the sensor shown in Fig. 9 is obtained by hooking high-precision masses from 0g to 3g in steps of 1 g, and we note the voltage values corresponding to each mass with a precision 0.1 mV. The curve response is not linear; it is rather parabolic in relation with the sensor sensitivity as a function of the distance between coils.

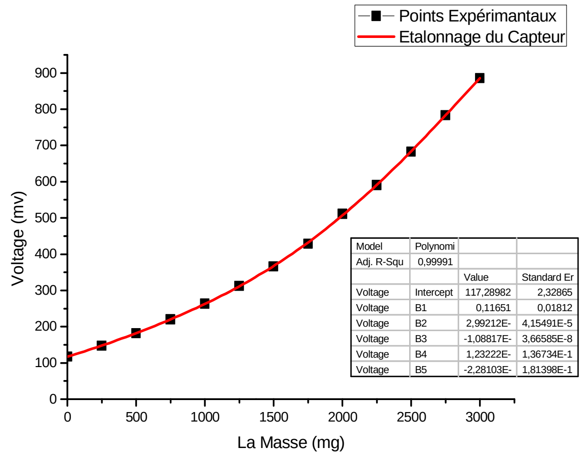

Fig. 9: Sensor response from 0g to 3g: V = f (V)

The fit polynomial of order 5, characterized by a standard deviation consistent with the experimental accuracy of the sensor ($\Delta V = \pm 0.1$ mV), appears suitable:

$$m(mg)_i = \sum_{j=0}^{5} B_j \times v_i^j \tag{14}$$

The coefficients of the polynomial fit are:
B_0=0.11651; B_1=2.99212E_{-5}; B_2=-1.08817E^{-8};
B_3=1.23222E^{-11}; B_4=-2.28103E^{-15}; B5=-2.28103E^{-15}

The characteristic equation:

$$m(mg) = -2.28103E^{-15} \times V5+ \quad -2.28103E^{-15} \times V4+ 1.23222E^{-11} \times V3+ -1.08817E^{-8} \times V2+ 2.99212E^{-5} \times V+ 0.11651 \tag{15}$$

Conversion the masses in displacement: The curve of Determination of the displacement d=f (v) obtained by conversion the masses in displacement while using the characteristic for spring k.

Table.1: The coefficient of Linear Thermal Expansion of Iron as a function of temperature from 30^{0}C at 96^{0}C

Time	**T**	**Voltage**	**Displacement d**	Δl	$\alpha_{Cop} \times 10^{-5}$
(min)	**(^{0}C)**	**(mv)**	**(mm)**	**(µmm)**	**(^{0}C^{-1})**
0	30	544.1	2.8402	0	---------
20	36	539.7	2.8552	14998.04	2.31795
40	42	534.6	2.8728	17548.66	2.71215
60	48	528.9	2.8926	19822.31	3.06354
80	54	522.5	2.9151	22519.67	3.48041
100	60	515.5	2.9401	24949.51	3.85594
120	66	507.9	2.9675	27464.93	4.2447
140	72	499.7	2.9976	30073.3	4.64783
160	78	490.9	3.0304	327819.3	5.06645
180	84	481.7	3.0652	348345.1	5.38367
200	90	472	3.1026	373504.1	5.7725
220	96	461.8	3.1425	399651.5	6.17661

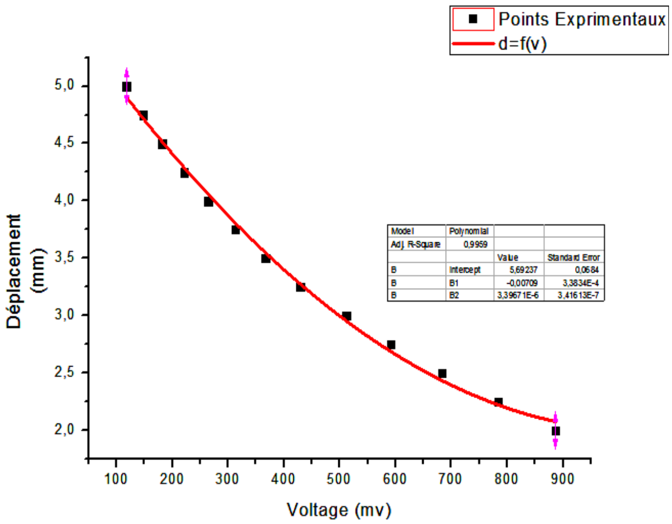

Fig. 10: Sensor response from 5mm to 2mm: d = f(V)

From the polynomial adjustment of Fig. 10, the relation of the mass as a function of the voltage corresponding to the experimental accuracy of our sensor is as follows:

d (mm) = 3.39671E-6 ×V2 - 0.00709×V + 5.69237 (16)

3.2 Measurement

We connected a rod of length (l=9.5 mm for iron; l=10.5 mm for copper or l=10.5 mm for aluminum) to a Hooke, which is attached to this sensor for determining the expansion caused by the temperature, we reports the different voltages corresponding at different temperatures. We deduced the table of the temperature as function to thermal expansion.

When the rod is connected to the sensor, the temperature is T=300 C and the voltage is : (V_1=745.1 mV for iron , V_1=544.1 mV for copper and V_1=715.5 mV for aluminum).The characteristic equation gives (d_{01}= 2.2953 mm for iron , d_{01}=2.8402 mm for copper and d01=2.3583 for Aluminum) , we considered that there's no dilation at T= 300 C and the original length of the rod is : l_0 = 9.5× 10+d_{01}≈97.3mm for iron , 107.84 mm for copper and 97.35 mm for aluminum). The linear expansion of the rod is calculated by the following relation:

$$\Delta l = d_{02} - d_{01} \qquad (17)$$

And the coefficient of Linear Thermal Expansion is measured by the following equation:

$$\alpha = \frac{\Delta L}{L_0 \times \Delta T} \qquad (18)$$

The data experimental is interfaced to the computer connected through the National Instruments multifunctional NI USB-6281 data acquisition module card which can support 16 analog inputs and 2 analog outputs channels with a voltage ranging between ±12 Volts. The sampling rate of the acquisition card module is 625Ks/S with 18 bit resolution. The graphical program written in LabVIEW is then linked to the set up through the acquisition module.

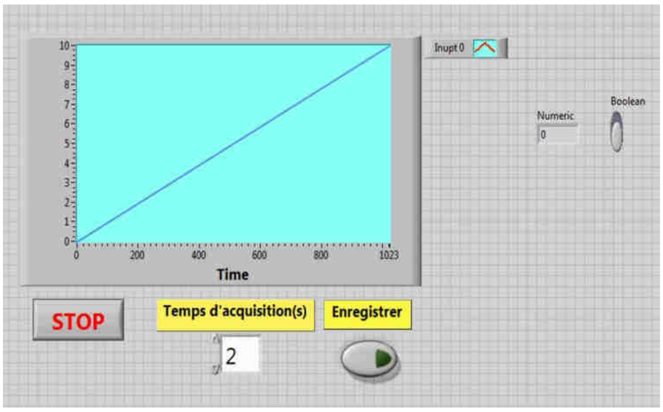

Fig. 11: The front panel of developed virtual system for linear thermal expansion measurement

Table.2: The coefficient of Linear Thermal Expansion of Copper as a function of temperature from 30^{0}C at 96^{0}C

Time	**T**	**Voltage**	**Displacement D**	Δl	$\alpha_{IR} \times$ **10-5**
(min)	**(^{0}C)**	**(mv)**	**(mm)**	**(µm)**	**(^{0}C^{-1})**
0	30	745.1	2.2953	0	---------
20	36	740.5	2.3047	9401.7	1.61043
40	42	735.3	2.3155	10801.1	1.85014
60	48	729.5	2.3278	12264.1	2.10074
80	54	722.9	2.3420	142336.8	2.43811
100	60	716	2.3572	151970.7	2.60313
120	66	708.5	2.3741	16885.4	2.89233
140	72	700.4	2.3928	186654.4	3.19723
160	78	691.9	2.4128	200664.7	3.43722
180	84	682.8	2.4349	220269.4	3.77303
200	90	673.5	2.4580	230922.9	3.95551
220	96	663.8	2.4827	247115.2	4.23287

Table.3: The coefficient of Linear Thermal Expansion of Aluminum as a function of temperature from 30^{0}C at 96^{0}C

Time	**T**	**Voltage**	**Displacement d**	Δl	$\alpha_{AL} \times$ **10^{-5}**
(min)	**(^{0}C)**	**(mv)**	**(mm)**	**(µm)**	**(^{0}C^{-1})**
0	30	715.5	2.3583	0	-------
20	36	707.2	2.3771	18737.26	3.20788
40	42	697.8	2.3989	21785.65	3.72978
60	48	687.3	2.4239	25044.78	4.28776
80	54	675.9	2.4519	28039.5	4.80046
100	60	663.5	2.4834	31501.54	5.39318
120	66	650.4	2.5179	34414.52	5.89189
140	72	636.6	2.5554	37514.39	6.4226
160	78	622.2	2.5959	40524.79	6.93799
180	84	607.2	2.6396	43711.27	7.48353
200	90	591.7	2.6864	46774.11	8.00789
220	96	575.7	2.7364	49994.89	8.5593

The Coefficient of Linear Thermal Expansion By this technique appear also to agree well with those reported previously in the literature [24-28].

V. CONCLUSION

The experiment presented in this work provides another method, based on a new IDS, to measure the metals dilatation coefficient very precisely and easily. The principle of the suggested electromagnetic dilatometer running rests on the fundamental laws of the electromagnetism, and the thermo-mechanical metals properties. It is constructed of a force-displacement converter and of a magnetic circuit which serves as displacement-voltage converter. The sensitivity of measurement is between 4mg/mV to 2.5mg/mV.

We have tested this measurement system on three metals which are; iron, copper and the aluminum. As a result, bring out the influence of the temperature on the metal. Therefore, we have observed that the obtained values of thermal dilatation coefficient by this technique are the same as well as those of the bibliography.

Finally, we can say that this device has proved its performance and its capacity for this practical application. The measurements of thermal expansion coefficient have allowed us to validate it experimentally. We think that this device can replace the traditional instruments, which remains in its details submitted to an industrial secret.

By contrast, user customers could find here a mean simple relatively, and inexpensive, robust, flexible, portable and reliable instrument to measure the thermal metals properties.

REFERENCES

[1] Dieter, George Ellwood, and David Bacon, Mechanical metallurgy, Vol. 3, New York: McGraw-Hill, 1986.

[2] Roy, Rustum, Dinesh K. Agrawal, and Herbert A. McKinstry. "Very low thermal expansion coefficient materials." Annual Review of Materials Science 19.1 (1989): 59-81.

[3] Case, John, and Amos Henry Chilver. Strength of materials and structures: an introduction to the mechanics of solids and structures. Elsevier, 2013.

[4] Pollock, H. M., and A. Hammiche. "Micro-thermal analysis: techniques and applications." Journal of Physics D: Applied Physics 34.9 (2001): R23.

[5] Fritschel, Peter. "Second generation instruments for the laser interferometer gravitational wave observatory (LIGO)." Astronomical Telescopes and Instrumentation. International Society for Optics and Photonics, 2003.

[6] White, G. K. "Measurement of thermal expansion at low temperatures." Cryogenics 1.3 (1961): 151-158.

[7] Nishikawa, T., et al. "Precise measurement method for temperature coefficient of microwave dielectric resonator material." Microwave Symposium Digest, 1987 IEEE MTT-S International. Vol. 1. IEEE, 1975.

[8] Kollie, T. G. "Measurement of the thermal-expansion coefficient of nickel from 300 to 1000 K and determination of the power-law constants near the Curie temperature." Physical Review B 16.11 (1977): 4872.

[9] Zhao, Jie-Hua, et al. "Measurement of elastic modulus, Poisson ratio, and coefficient of thermal expansion of on-wafer submicron films." Journal of applied physics 85.9 (1999): 6421-6424.

[10] Tech Note TN-504-1, "Strain Gage Thermal Output and Gage Factor Variation with Temperature", Vishay Micro-Measurements, January 2005.

[11] Kim S., Kim J. H., Lee J. K., Jarng S. S., "Measurement of thermal expansion coefficients by electronic speckle pattern interferometry at high temperature", J. Mater. Sci. Lett., vol. 16, pp. 1753-56, 1997.

[12] Dudescu C., Naumann J., Stockmann M., Nebel S., "Characterisation of thermal expansion coefficient of anisotropic materials by electronic speckle pattern interferometry", Strain, vol. 42 (3), pp.197–205, 2006.

[13] Lee C.C., Tien C.L., Sheu W.S., Jaing C.C., "An apparatus for the measurement of internal stress and thermal expansion coefficient of metal oxide films", Rev. Sci. Instrum., vol. 72 (4), pp.2128–2133, 2001.

[14] Bing P., Hui-min X., Tao H., Asundi A., "Measurement of coefficient of thermal

[15] Ho, Cho Yen, and Richard Erwin Taylor, eds. Thermal expansion of solids. Vol. 4. ASM international, 1998.

[16] American Society for Testing and Materials 2011 ASTM E 228-11.

[17] American Society for Testing and Materials 2010 ASTM E 289-04

[18] James J. D., Spittle J. A., Brown S.G.R., Evans R.W., "A review of measurement techniques for the thermal expansion coefficient of metals and alloys at elevated temperatures", Meas. Sci. Technol., vol. 12, pp. R1–R15, 2001.

[19] Amine Benabdellah, Zakarya Abbassi, Abdelrhani Nakheli, "New Electromagnetic Force-Displacement Sensor", International Journal of Electrical and Computer Engineering (IJECE), Vol 6, No 2, (2015).

[20] Z. Abbassi, A. Benabdellah, A. Nakheli, New Electromagnetic Force Sensor: Measuring the Density of Liquids, International Journal of Research in Engineering and Technology, Vol-03 Iss-09, Sep-2014, pp.83-90.

[21] J.E. LENZ; A Review of Magnetic Sensors;IEEE, VOL. 78, NO. 6, JUNE 1990

[22] J. Lenz, A.S. Edelstein; Magnetic Sensors and Their Applications; IEEE SENSORS JOURNAL, VOL. 6, NO. 3, JUNE 2006

[23] S. Tumanski; Induction Coil Sensors – a Review; Meas. Sci. Technol.18 (2007) R31–R46

[24] Wilson, A. J. C. "The thermal expansion of aluminum from 0 to 650 C." Proceedings of the Physical Society 53.3 (1941): 235.

[25] James, J. D., et al. "A review of measurement techniques for the thermal expansion coefficient of metals and alloys at elevated temperatures." Measurement Science and Technology 12.3 (2001): R1.

[26] Touloukian, Y. S., et al. Thermophysical Properties of Matter-the TPRC Data Series. Volume 12. Thermal Expansion Metallic Elements and Alloys. Thermophysical and electronic properties information analysis center lafayette in, 1975.

[27] is available online by:

http://www.simulationmateriaux.com/ComportementMecanique/comportement_mecanique_Liste_coefficients_de_dilatation_thermique.php

[28] is available online by : http://www.engin.brown.edu/organizations/EWB/GISP/Callster%20%20chapter_17.pdf

[29] Z. Ezzouine and A. Nakheli, A Simple Method for Determining Thermal Expansion Coefficient of Solid Materials with a Computer-aided Electromagnetic Dilatometer Measuring System ,Sensors & Transducers, Vol. 190, Issue 7, pp. 86-91, July 2015.